Self-Affine Fractal Vapour-Deposited Gold Surfaces Characterization by Scanning Tunnelling Microscopy

View the article online for updates and enhancements.

Self-Affine Fractal Vapour-Deposited Gold Surfaces Characterization by Scanning Tunnelling Microscopy.

R. C. Salvarezza (*), L. Vázquez (**), P. Herrasti (***), P. Ocón (***)
J. M. Vara (***) and A. J. Arvia (*)

(*) *Instituto de Investigaciones Fisicoquímicas Teóricas y Aplicadas* (*INIFTA*)
Sucursal 4, Casilla de Correo 16, 1900 La Plata, Argentina
(**) *Instituto de Ciencia de Materiales, CSIC, D.pto Física Aplicada C-XII*
Universidad Autónoma de Madrid (*UAM*) - *28049 Madrid, Spain*
(***) *D.pto Química Física Aplicada C-II, Universidad Autónoma de Madrid*
28049 Madrid, Spain

Abstract. – The morphological evolution of the surfaces of gold deposits grown from the vapour on smooth glass under nonequilibrium conditions and incident angle near substrate normal is studied at the nanometer level by scanning tunnelling microscopy. For an average film thickness equal to or greater than 500 nm, the interface thickness (ξ) reaches a steady state. Under these conditions, ξ depends on the scan length (L) as $\xi \propto L^{\alpha}$ with $\alpha = 0.35 \pm 0.05$ for $L > d_{s}$, where d_{s} is the columnar size, and $\alpha = 0.89 \pm 0.05$ for $L < d_{s}$. These results indicate that the growing surface spontaneously reaches a steady state and it can be described as a self-affine fractal. The value of α for $L > d_{s}$ agrees with the prediction of ballistic deposition models without restructuring, whereas that for $L < d_{s}$ exceeds the prediction of ballistic models including restructuring.

A relatively large number of physical and chemical processes under nonequilibrium conditions are related to the development of complex structures involving rough surfaces. This is the case of metal deposition from the vapour where either atoms or molecules are incorporated to the growing deposit following near-ballistic trajectories [1]. These deposits exhibit a columnar structure [2] with interfaces which have been described either as self-similar [3] or as self-affine fractals [4]. Ballistic deposition models [5,6] have been preferentially used for describing the evolution and the properties of vapour-deposited metal films, although continuum models such as the grass and those based on the Huygens principle have also been proposed [7,8]. Thus, large-scale computer simulation of ballistic models generates compact structures with self-affine fractal surfaces [8], whereas continuum models predict compact structures with self-similar surfaces [9]. The fact that in all these cases the growing surfaces must reach a steady state characterized by universal fractal properties has been interpreted in terms of the self-organized criticality mechanism [10]. The possibility of checking the validity of the different models for surface growth has been hampered by the

lack of high-quality experimental data on thin-film morphology and evolution. Scanning tunnelling microscopy (STM) appears as an adequate technique for this purpose due to its high 3D resolution and nondestructive character [11].

Several attempts to characterize vapour-deposited metal surfaces as fractals from STM imaging analysis have been recently reported [12-15]. In this letter we report on STM measurements of vapour-deposited gold films grown under nonequilibrium conditions covering a relatively broad range of film thicknesses. The dynamic scaling of surface growth [4] applied to STM data resulting from films under steady-state conditions allows us to prove the self-affine character of the surface of these films, and the validity of ballistic models for describing some aspects of vapour-deposited film morphology.

Gold films were grown on smooth glass substrates previously cleaned in an ultrasonic bath by sequentially using water, trichloroethylene, acetone and ethanol. The glass substrate was characterized by atomic-force microscopy imaging which revealed a substrate corrugation less than 0.5 nm [16]. Gold deposits were prepared in an evaporator chamber. The angle between the direction of incident particles and the substrate normal was set in the $(2 \div 25)$ degrees range. The following evaporator chamber conditions were applied pressure, $P = 10^{-4}$ Torr, average deposit growth rate, $v = 30 \, nm \, s^{-1}$, and substrate temperature, $T = 298$ K. The average film thickness, δ $(30 \, nm < \delta < 1000 \, nm)$ was measured with a profilometer.

The STM measurements were performed in air using platinum tips. The microscope was calibrated by imaging highly oriented pyrolytic graphite (HOPG). To minimize occasional tip geometric artifacts different tips were used, although no influence of the tip shape was detected in our experimental data. Typical STM conditions were a bias voltage of 0.05 V (tip (+)) at a constant current of $(1 \div 2)$ nA. Data were acquired in a fully automated work station and stored as digitized images with 256×256 pixels.

The surface of the vapour-deposited gold films for $\delta = 850$ nm is depicted in fig. 1. The STM images reveal rounded top columns with size $d_s \simeq 38$ nm, and remified voids. For a given film thickness δ, the r.m.s. roughness measured from an STM image with total scan length S, ξ_{stm}, increases with S until a saturation value, ξ_{stm}^0, is reached [17]. In fig. 2 these ξ_{stm}^0 values for four vapour-deposited gold films are plotted. For small δ values ξ_{stm}^0 increases indicating that the film becomes rougher during growth, whereas for $\delta \geqslant 500$ nm a saturation value is obtained, independent of δ, as it corresponds to a surface which has reached a steady-state roughness.

To characterize the fluctuating interfaces of vapour-deposited gold, the dynamic scaling of surface growth was applied [18,19]. In this case, for a sample of lateral dimension L, the surface width in the i-direction, $\xi^i(L)$, is defined as the mean-square average roughness given by

$$\xi^i(L) = [1/L \sum [h_j - \boldsymbol{h}]^2]^{1/2} \, , \tag{1}$$

where h_j is the deposit height measured along the i-direction at the j-position, and $\boldsymbol{h}$ is the average height of the sample. Besides, ξ and L are related through the equation

$$\xi^i(L, h) \propto L^\alpha f(x) \, , \tag{2}$$

where $f(x) = \boldsymbol{h}/L^\gamma$. The function $f(x)$ has the following properties: $f(x) = $ const for $x \Rightarrow \infty$, and $f(x) = x^{\alpha/\gamma}$ for $x \Rightarrow 0$. Thus, after a certain critical thickness (time), ξ^i reaches a steady state, and eq. (2) becomes

$$\xi^i(L) \propto L^\alpha \, . \tag{3}$$

The preceding dynamic scaling concepts can be applied to STM data derived for the vapour-deposited gold surfaces as $\xi^i = \xi_{stm}^i$, *i.e.* ξ_{stm}^i is the mean-square average roughness
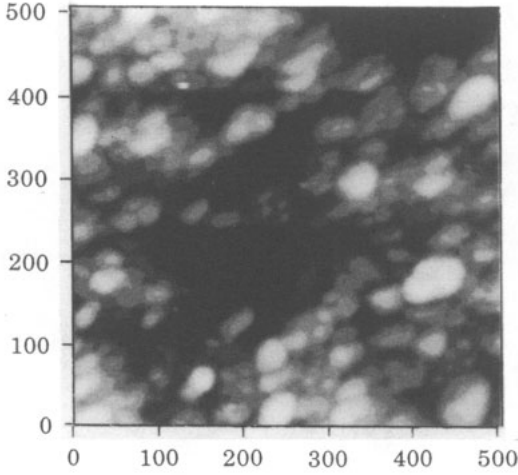
Fig. 1.   Fig. 2.

Fig. 1. – STM gray-scale top-view image ((505×505) nm^2) of a vapour-deposited gold film of average thickness $\delta = 850$ nm. The total height scale difference is 17 nm.

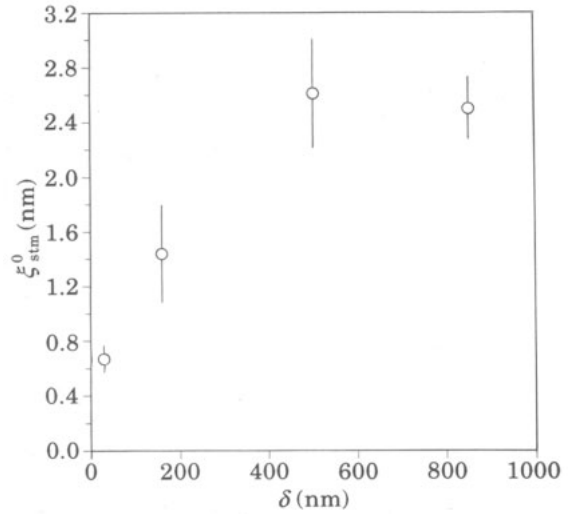Fig. 2. – Dependence of ξ^0_{stm}, the limiting value of the experimental ξ_{stm} values, on δ, the average film thickness of vapour-deposited gold films, obtained with more than 90 STM images.

determined by the STM scans in the i-direction ($i = x, y$). Accordingly, we have determined the r.m.s. value of the fluctuations of h over each STM scan segment of length L_s along the x and y directions after standard plane correction. More explicitly, we have used

$$\xi^i_{\text{stm}}(L_s) \propto \left[1/L_s \sum [h_j - \boldsymbol{h}_s]^2 \right]^{1/2} \tag{4a}$$

and

$$\xi^i_{\text{stm}} \propto L_s^{\alpha} \tag{4b}$$

where $\boldsymbol{h}_s$ is the average height of the surface profile of length L_s in either the x- or the y-direction. For each scan 250 pairs of data points (L_s, ξ^i_{stm}) have been obtained, L_s being varied from $S/64$ to S. Finally, for each L_s the corresponding ξ^i_{stm} value represents the average value resulting from 256 scans of the same image. In this way the log ξ^x_{stm} *vs.* log L_s plot for an STM image of a gold deposit ($\delta = 850$ nm) with $S = 507$ nm has been obtained (fig. 3a)). The plot shows two linear regions with a crossing point at log $L_s = 1.6$, and a saturation region for log $L_s > 2.6$. The slopes of the straight lines are 0.73 ± 0.1 for log $L_s < 1.6$, and 0.30 ± 0.06 for log $L_s > 1.6$.

The evaluation of α was also made in the y-direction (fig. 3b)). In this case, the two linear regions can also be observed with a crossing point at log $L_s = 1.55$. However, the plots obtained in the y-direction sometimes presented anomalous or bigger α values as Mitchell *et al.* have reported [13]. This can be due to drift effects or to a noise probably arising from low-frequency mechanical vibrations, both more evident in the slow scan direction. Consequently, those measurements made in the fast x-direction have been always considered to estimate α.

Although for computer-simulated fractals data covering 4-5 orders of magnitude in scale length are usually required for logarithmic fittings [1], for experimental systems the
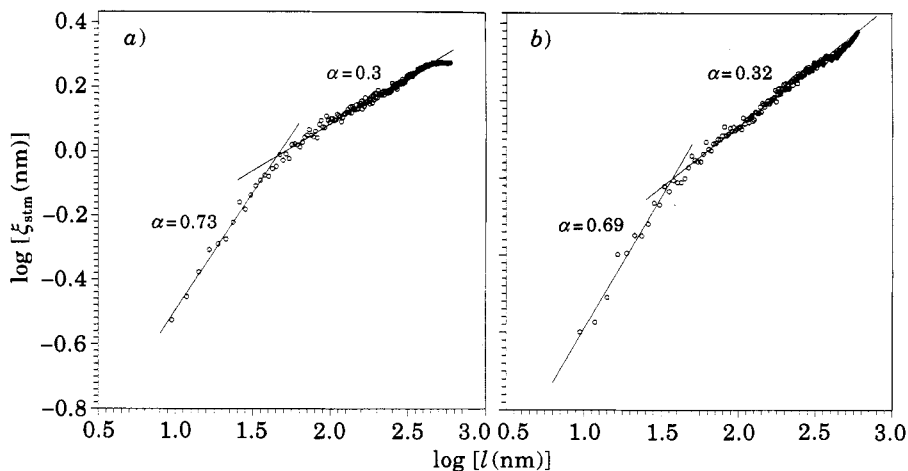
Fig. 3. – log ξ^i_{stm} vs. log L_s plots calculated from STM scans ($S = 507$ nm) in the x-direction (a)) and in the y-direction (b)) resulting for a vapour-deposited gold film of $\hat{c} = 850$ nm.

situation is less ambitious as frequently the fractal behaviour is restricted to a certain scale length. Accordingly, fractal structures of real objects are characterized by log-log plots covering at least one-order-of-magnitude scale length thereabouts [20]. The latter situation is satisfied for both linear portions in the log ξ^i_{stm} vs. log L_s shown in fig. 3.

The capability of the method proposed for calculating the value of α from STM images has been tested by analysing several computer-simulated self-affine fractal surfaces generated on a 256×256 square grid using the successive random addition algorithm [21]. It was found [22] that α values were underestimated by $(5 \div 20)\%$ for $\alpha > 0.6$, as has also been reported for different methods [13,15]. Sometimes saturation regions as that observed in fig. 3a) appeared when these simulated profiles were analysed by the proposed method. However, at present, we consider more probable that this saturation is not an artifact. This idea is supported experimentally as a saturation roughness region, in the range of the
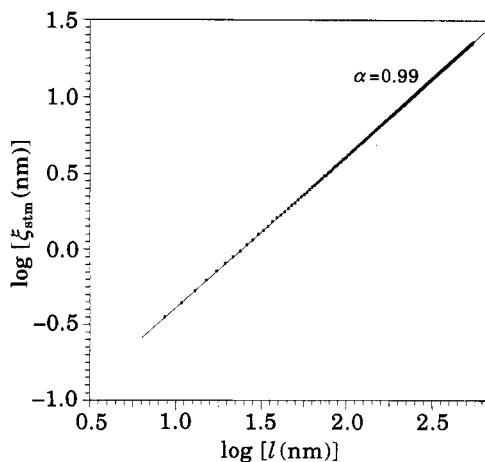

Fig. 4. – log ξ^i_{stm} vs. log L_s plots calculated from STM scans ($S = 859$ nm) in the x-direction obtained for a gold single crystal.

micron, was also found when these films were analysed by other methods [17, 23]. Also, it should be noted that the existence of a high cut-off in these films is evident as they appear smooth when they are imaged by SEM. Furthermore, for checking purpose the method was also applied to STM images of spherical gold single-crystal surfaces. These images reveal large terraces with steps smaller than 1 nm height, and $\alpha \sim 1$, as should be expected for a nonfractal surface (fig. 4).

The average value of α resulting from 12 different STM images of an evaporated gold film with $h = 850$ nm and 27 nm $< S < 605$ nm is $\alpha = 0.74 \pm 0.05$ for $\log L_\mathrm{s} < 1.6$, and $\alpha = 0.35 \pm 0.05$ for $\log L_\mathrm{s} > 1.6$. If we take into account the results obtained for computer-simulated fractal surfaces, the true value of α for $\log L_\mathrm{s} < 1.6$ is 0.89 ± 0.05 whereas, as no significant correction is required for $\alpha < 0.6$, when $\log L_\mathrm{s} > 1.6$ the right α value is 0.35 ± 0.05.

It should be noted that the value $L_\mathrm{s} = 38$ nm ($\log 38 \simeq 1.6$) lies very close to the average columnar size of the deposit. This fact means that for $L_\mathrm{s} < d_\mathrm{s}$ the deposit surface approaches the behaviour of a smooth surface, whereas for $L > d_\mathrm{s}$ it behaves as a rough self-affine fractal surface. In fact, there is a trend of columnar surfaces to become rather smooth as the surface diffusion of atoms contributes to eliminate irregularities smaller than the diffusion length of moving particles, the latter being close to the d_s value [9].

The value $\alpha \simeq 1/3$ obtained in the present work for $L_\mathrm{s} > d_\mathrm{s}$ has been recently reported for evaporated gold films by using a different method [17]. It should be noted that values of α ranging between $0.35 \div 0.64$, *i.e.* approaching to some extent $\alpha = 1/3$, have been obtained for silver deposited on different substrates at 80 K from adsorption and X-ray reflectivity data [24].

Let us consider the values of α derived in this work in relation to the ballistic models for particle deposition. Thus, for $L_\mathrm{s} > d_\mathrm{s}$ the experimental value $\alpha = 0.35 \pm 0.05$ agrees with $\alpha = 1/3$ resulting from either large-scale computer simulations of 3D deposits generated by the Eden [4] or the ballistic models at incident angles near the normal to the substrate without surface restructuring [6, 19]. Furthermore, the experimental data agree reasonably with Halpin-Healey's predictions for interface growth [18]:

$$\alpha = (5 - d)/6, \tag{5}$$

where d is the space dimension.

For $L_\mathrm{s} < d_\mathrm{s}$ the value $\alpha = 0.89 \pm 0.05$ indicates the development of a smoother columnar surface presumably assisted by the relatively high gold surface atom mobility at 298 K. This value exceeds $\alpha = 0.67$ resulting from continuum models incorporating surface reconstruction [25] and it is also higher than that reported for a sputter-deposited gold film from STM data using the Fourier-transform analysis [13]. For the latter the square amplitude *vs.* frequency plot showed two distinct regimes, although the analysis of the data was limited to small scale lengths.

The ballistic models cannot predict the appearance of two regimes of growth as experimentally observed. Thus, for ballistic models without surface restructuring irregularities at the growing surface appear at the atomic scale, and the exponent $\alpha = 1/3$ can be observed at all scale lengths [6]; whereas for real vapour gold surfaces those irregularities disappear at a scale length smaller than the columnar size, leading to $\alpha = 0.89 \pm 0.05$. Otherwise, when surface diffusion is included, ballistic deposition models predict higher α values [26], and continuum models yield $\alpha = 0.67$ [25] for all scale lengths, in contrast to the real vapour gold surface exhibiting $\alpha = 0.35 \pm 0.05$ at a scale length larger than the columnar size. In fact, the present data indicate that the ballistic models without surface restructuring are valid for $L_\mathrm{s} > d_\mathrm{s}$, whereas continuum models with surface diffusion lead to α values smaller than that obtained in our work.

In conclusion, the fractal character of metal surfaces has been determined at the nanometer level from STM data by using the dynamic-scaling approach for surface growth. Two distinct regimes for the development of vapour-deposited gold surfaces characterized by $\alpha = 0.35 \pm 0.05$ and $\alpha = 0.89 \pm 0.05$ for $L_s > d_s$ and $L_s < d_s$, respectively, were observed. In our opinion, the present data provide experimental evidence for the self-affine character of gold surfaces grown from the vapour far from equilibrium conditions. The value $\alpha = 1/3$ for $L_s > d_s$ agrees with those resulting from computer simulations of ballistic models without restructuring at incident particle angles near the substrate normal; whereas $\alpha \simeq 0.9$ for $L_s < d_s$ exceeds the predictions of continuum models including surface diffusion.

$$* * *$$

REFERENCES

[1] MEAKIN P., *Crit. Rev. Solid State Mat. Sci.*, **13** (1987) 147.
[2] MOVCHAN B. and DEMCHISHIN A. V., *Phys. Met. Metallogr.*, **28** (1969) 83.
[3] MESSIER R. and YEHODA J. E., *J. Appl. Phys.*, **58** (1986) 3739.
[4] VICSEK T., *Fractal Growth Phenomena* (World Scientific, Singapore) 1989.
[5] VOLD J. M., *J. Colloid Sci.*, **14** (1959) 168.
[6] MEAKIN P., RAMANLAL P., SANDER L. M. and BALL R. C., *Phys. Rev. A*, **34** (1986) 509; KRUG J. and MEAKIN P., *Phys. Rev. A*, **43** (1991) 900.
[7] KARUNASIRI R. P. U., BRUINSMA R. and RUDNICK J., *Phys. Rev. Lett.*, **62** (1989) 788.
[8] TANG C., ALEXANDER S. and BRUINSMA R., *Phys. Rev. Lett.*, **64** (1990) 772.
[9] BALES G. S., BRUINSMA R., EKLUND E. A., KARUNASIRI R. P. U., RUDNICK J. and ZANGWILL A., *Science*, **249** (1990) 264.
[10] BAK P., TANG C. and WIESENFELD K., *Phys. Rev. Lett.*, **59** (1987) 381.
[11] BINNING G., ROHRER H., GERBER CH. and WEIBEL E., *Phys. Rev. Lett.*, **49** (1982) 57.
[12] PFEIFER P., YU Y. J., COLE M. W. and KRIM J., *Phys. Rev. Lett.*, **62** (1989) 1997.
[13] MITCHELL M. W. and BONNEL D. A., *J. Mater. Res.*, **5** (1990) 2244.
[14] EKLUND E. A., BRUINSMA R., RUDNICK J. and WILLIAMS R. S., *Phys. Rev. Lett.*, **67** (1991) 1759.
[15] MILLER S. and REIFENBERGER R., *J. Vac. Sci. Technol. B*, **10** (1992) 1203.
[16] HUANG W. A., private communication.
[17] HERRASTI P., OCÓN P., VÁZQUEZ L., SALVAREZZA R. C., VARA J. M. and ARVIA A. J., *Phys. Rev. A*, **45** (1992) 7440.
[18] FAMILY F., *Physica A*, **168** (1990) 561.
[19] MEAKIN P. and KRUG J., *Europhys. Lett.*, **11** (1990) 7.
[20] KAYE B. H., in *The Fractal Approach to Heterogeneous Chemistry*, edited by D. AVNIR (John Wiley & Sons, New York, N.Y.) 1990.
[21] VOSS R. F., in *Fundamental Algorithms in Computer Graphics*, edited by R. A. EARNSHAW (Springer-Verlag, Belin) 1985.
[22] VÁZQUEZ L., SALVAREZZA R. C., HERRASTI P., OCÓN P., VARA J. M. and ARVIA A. J., presented at the *IVC-12/ICSS-8, 12-16 October 1992, The Hague, The Netherlands.*
[23] GOMEZ RODRIGUEZ J. M., ASENJO A., SALVAREZZA R. C. and BARO A., *Ultramicroscopy*, in press.
[24] CHIARELLO R., PANELLA V., KRIM J. and THOMPSON C., *Phys. Rev. Lett.*, **67** (1991) 3408 and references therein.
[25] LAI Z. W. and DAS SARMA S., *Phys. Rev. Lett.*, **66** (1991) 2348.
[26] MEAKIN P. and JULLIEN R., *Phys. Rev. A*, **41** (1990) 983.